

# Correlations between the crystallographic texture and grain boundary character in polycrystalline materials

R. Edwin García <sup>a,\*</sup>, Mark D. Vaudin <sup>b</sup>

<sup>a</sup> *Materials and Electrical Engineering, School of Materials Engineering, Purdue University, 501 Northwestern Avenue, West Lafayette, IN 47907-2044, USA*

<sup>b</sup> *Ceramics Division, National Institute of Standards and Technology, Gaithersburg, MD 20899-8500, USA*

Received 11 November 2006; received in revised form 9 June 2007; accepted 12 June 2007

Available online 21 August 2007

## Abstract

A method is presented to determine the misorientation probability distribution function in polycrystalline materials based on a known, analytical or numerical, representation of the associated orientation probability distribution function, i.e., texture. The proposed formulation incorporates the local grain-to-grain orientation correlations by combining local or macroscopic statistical information, and finds a natural interpretation through the well-known stereographic projection (pole-figure) representation. The proposed formulation distinguishes between antiparallel crystallographic orientations, as well as cone-angle and polar angle misorientations. For fiber-textured samples, it is quantitatively shown that highly oriented samples are equivalent to polycrystals with a high density of low-angle misorientations, while completely random (untextured) materials are equivalent to microstructures with a high probability of large-angle misorientations.

© 2007 Acta Materialia Inc. Published by Elsevier Ltd. All rights reserved.

*Keywords:* Texture design; Grain boundary engineering; Grain boundaries; Polycrystals

## 1. Introduction

The microstructure of polycrystalline materials is a result of local grain–grain interface and bulk interactions. Such interactions encourage specific grain boundary misorientations with respect to others; for example, in the absence of additional driving forces, low interfacial energy boundaries are favored with respect to interfaces with large interface tension, thus promoting the appearance of low-angle misorientations with respect to high-angle values. In many cases, however, the kinetic mechanisms that control the mobility of the interfaces lead to the appearance of a set of metastable states that locally favor high-angle misorientations over low-angle values [1,2].

Recently, texture and interface engineering have been developed as two innovative approaches to take advantage

of the microstructural interactions in a continuing effort to improve material response and reliability. Texture design, in particular, explores the effect of the anisotropy of the single-crystal properties of individual phases on the macroscopic response of polycrystalline materials. The approach searches for thermodynamic conditions and kinetic processes that will favor the orientation of one or more crystallographic directions along a laboratory reference system direction [3]. In turn, interface engineering is an emerging methodology whose goal is to specify those crystallographic planes and interfacial misorientations that improve on the macroscopic properties and reliability of materials.

For both methodologies, significant advances in experimental and computing power have been achieved throughout the last thirty years, yielding detailed information of the materials and their associated intrinsic properties. These advances have made it possible to collect and analyze large quantities of experimental data and have provided the opportunity for accurate material characterization and

\* Corresponding author.

E-mail address: [redwing@purdue.edu](mailto:redwing@purdue.edu) (R.E. García).

improvement. Diffraction techniques have developed from specifying elementary information such as crystal structure to determining a myriad of microstructural details such as grain morphology, volume fractions and spatial distribution of stable thermodynamic phases, plastic strain fields, orientation distribution of the crystallographic axes, etc.

In the present context, accurate mathematical representations of the statistical distributions and local grain–grain correlations of the crystallographic orientations is critical for the understanding of material response [4–6]. Previous work has established statistical descriptions for the disorientation of randomly oriented (untextured) cubic polycrystalline systems [8]. Other approaches have applied two- and three-point correlation functions to characterize the angle between two crystallographic directions of neighboring grains, specify the average misorientation, and address the effect of grain clustering in experimentally characterized material systems [9]. These approaches applied two-point statistics to specify correlation functions by starting from experimental results [10]. More recently, numerical Monte Carlo-based studies have shed some light on the relationships between crystallographic texture and the misorientation of grains [7]. Schuh et al. extensively developed this idea and presented numerical results where correlation lengths and percolation distances of specific types of grain boundaries are quantified [11–13]. The present paper establishes analytical relationships between a known statistical representation of the crystallographic orientation distribution function (ODF) of a polycrystal and the associated misorientation distribution function (MDF). The description presented in this manuscript shows that an ODF imposes constraints on the MDF. Furthermore, in the limit of morphologically isotropic polycrystals, it is demonstrated that an MDF representation of a solid is equivalent to an ODF characterization; therefore, the concepts and ideas developed through interface engineering are applicable in texture design approaches. While the framework described herein is amenable to directly incorporate the local grain–grain orientation correlations, topological constraints imposed on the misorientation probability distribution, such as those found at grain corners, are not explicitly included. An application to fiber-textured solids is presented. The formulation presented in this paper is independent of the specific representation of the rotation; however, in what follows, orientations are represented in terms of a set of Euler angles  $\phi_1$ ,  $\Phi$ , and  $\phi_2$ , as described by Bunge [14] (see Fig. 1a).

## 2. Theoretical framework

### 2.1. Geometrical construction

Texture is present in a polycrystalline material if a specific crystal direction of an individual phase, e.g., the  $c$ -axis of a grain or the  $\{111\}$  pole of a face-centered cubic metal, has a greater-than-random probability of alignment with respect to a laboratory reference system direction.

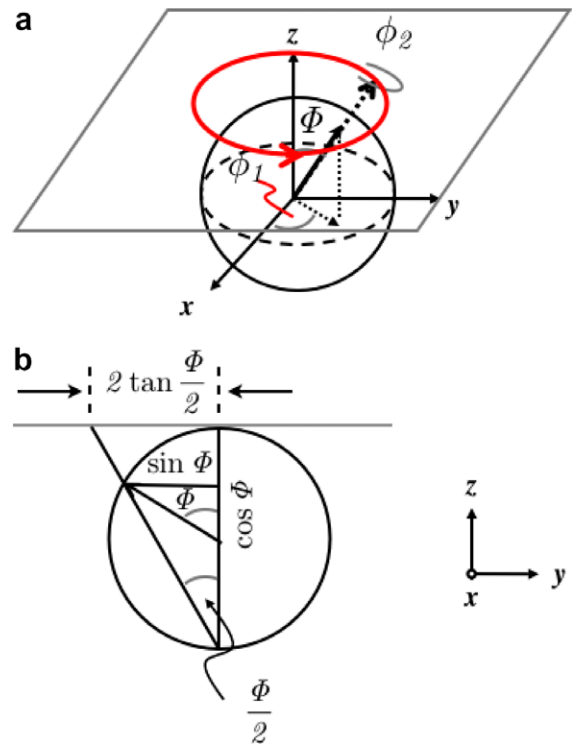


Fig. 1. (a) Three-dimensional representation of the rotation of a crystallographic axis with respect to a laboratory reference system,  $x$ ,  $y$ ,  $z$ . (b) Side view of a stereographic projection of a three-dimensionally oriented crystallographic axis. In-plane radial direction corresponds to  $2\tan(\Phi/2)$ , while angular direction corresponds to polar direction,  $\phi_1$ . The sphere possesses a unit size radius.

Mathematically, texture is quantified through a function,  $P_O(\vec{t}_O, \vec{g}, \vec{x})$ , which determines the probability of finding a crystallographic orientation between the orientations  $\vec{g}$  and  $\vec{g} + d\vec{g}$ , at a specified location  $\vec{x}$ .  $\vec{t}$  is the vector of parameters that characterizes the MDF.

An important piece of information not traditionally included in macroscopic material characterization methods is the local grain-to-grain orientation correlation. Such information can be easily extracted from orientation mapping measurements, e.g., electron backscatter diffraction (EBSD) [15,16], and readily summarized through a misorientation probability distribution function,  $P_M(\vec{t}_M, \hat{n}_{ij}, \Delta\vec{g}_{ij})$ , where

$$\Delta\vec{g}_{ij}(\Delta\phi_1, \Delta\Phi, \Delta\phi_2) = \vec{g}^{-1}(\phi_{1,i}, \Phi_i, \phi_{2,i}) \cdot \vec{g}(\phi_{1,j}, \Phi_j, \phi_{2,j}) \quad (1)$$

is the misorientation between the  $i$ th and the  $j$ th neighboring grains.  $\{\Delta\phi_1, \Delta\Phi, \Delta\phi_2\}$  defines the Euler angles describing the orientation of the principal axes of the  $j$ th grain from the reference system of the  $i$ th grain. Similarly,  $\hat{n}_{ij}$  corresponds to the normal separating the interface between the  $i$ th and the  $j$ th grain, and  $\vec{t}_M$  is the vector of texture parameters that characterizes the MDF.

The character of an interface in a polycrystal is determined by specifying five geometrical parameters: the three

Euler rotation angles that characterize the misorientation matrix,  $\Delta\vec{g}_{ij}(\Delta\phi_1, \Delta\Phi, \Delta\phi_2)$ , plus two components of the normal to the interface,  $\hat{n}_{ij}$ , separating the two abutting grains. Thus, for a fixed interface normal,  $\hat{n}_{ij}$ ,  $P_M$  determines the probability of finding a grain misoriented between  $\Delta\vec{g}_{ij}$  and  $\Delta\vec{g}_{ij} + d\Delta\vec{g}_{ij}$ . Similarly, for fixed misorientation,  $P_M$  measures the probability of finding an interface whose normal is between  $\hat{n}_{ij}$  and  $\hat{n}_{ij} + d\hat{n}_{ij}$ . Polycrystals showing some degree of morphological texture will favor the occurrence of a subset of interfaces. In contrast, for morphologically isotropic microstructures of homogeneous grain size, the MDF is independent of the interface normal,  $\hat{n}_{ij}$ , because every interface normal is equally probable, i.e.,  $P_M = P_M(\vec{t}_M, \Delta\vec{g}_{ij})$ .

Fiber texture is present if a specific crystallographic direction of each grain, known as the preferred orientation direction or textured direction, has a different-than-random probability of alignment in a particular laboratory reference system direction, the fiber or texture axis, but the orientation of each grain around its textured direction is random. Thus, the orientations of the grains have axial symmetry around the texture axis. Set the  $z$ -axis of the laboratory reference system parallel to the texture axis of a polycrystal and propose the separation of variables:

$$P_O(\vec{t}_O, \phi_1, \Phi, \phi_2) = P_f(\vec{t}_\Phi, \Phi) P_p(\vec{t}_{\phi_1}, \phi_1) P_b(\vec{t}_{\phi_2}, \phi_2) \quad (2)$$

$P_f(\vec{t}_\Phi, \Phi)$  is defined as the fiber texture contribution and  $P_p(\vec{t}_{\phi_1}, \phi_1)$ , as the polar contribution. In fiber-textured solids, the texture direction is unaffected by the value of  $\phi_2$ ; therefore,  $P_b(\vec{t}_{\phi_2}, \phi_2)$  provides no contribution to modulate the ODF and is set to 1 for the remainder of this paper.  $\Phi$ , the angle between the texture axis and the textured direction, will be termed the cone angle.

The contributions from the different components of the ODF are graphically represented through a stereographic

projection. If the textured crystallographic direction (see Fig. 1b) makes a cone angle,  $\Phi$ , with the  $z$ -axis of the laboratory reference system, its stereographic projection will map into a circle of radius  $2\tan(\Phi/2)$  as the polar angle  $\phi$  takes values between 0 and  $2\pi$ . Similarly, a fixed value of polar angle,  $\phi_1$ , of a  $c$ -axis with the  $x$ -axis of the laboratory reference system will project into the stereographic projection plane as a line that makes an angle  $\phi_1$  with the  $x$ -axis of the plane, as  $\Phi$  takes values between  $-\pi$  and  $\pi$ .

Therefore, from Eq. (2), a solid possessing only fiber texture, i.e.,  $P_O(\vec{t}_O, \vec{g}(\phi_1, \Phi, \phi_2)) = P_f(\vec{t}_\Phi, \Phi)$ , produces contributions to the distribution of crystallographic orientations whose only variations on the projection plane are in the radial direction. Similarly, a polycrystal possessing only polar contributions to texture about a polar axis, i.e., for the case  $P_O(\vec{t}_O, \vec{g}(\phi_1, \Phi, \phi_2)) = P_p(\vec{t}_{\phi_1}, \phi_1)$ , produces a pole-figure where the two-dimensional probability of orientation reaches its maxima at specific two-dimensional polar angles. The stereographic projection of an ODF of a hypothetical polycrystal with fiber texture is shown in Fig. 2. Here, the locus of points of accessible cone angles on the stereographic projection plane is represented as an annulus (or ring) of radius  $2\tan(\Phi/2)$  and thickness  $2\tan((\Phi + \delta\Phi/2)/2) - 2\tan((\Phi - \delta\Phi/2)/2) = 2\sin(\delta\Phi/2)/(\cos(\delta\Phi/2) + \cos\Phi)$ , so orientations outside the dashed area of the ring have a zero probability of occurring. From the reference system of an arbitrary grain marked as  $\times$ , the possible misorientations of the grains neighboring  $\times$  are given by those Euler angle values that can be sampled within the area spanned by the ring, as in Fig. 2a. Graphically, the proposed situation is equivalent to translating  $\times$  to the center of the projection plane (see Fig. 2b). The orientation distribution remains unaltered and the relative misorientations between the grains are unchanged. Thus, in the reference system of  $\times$ , the only grains that are

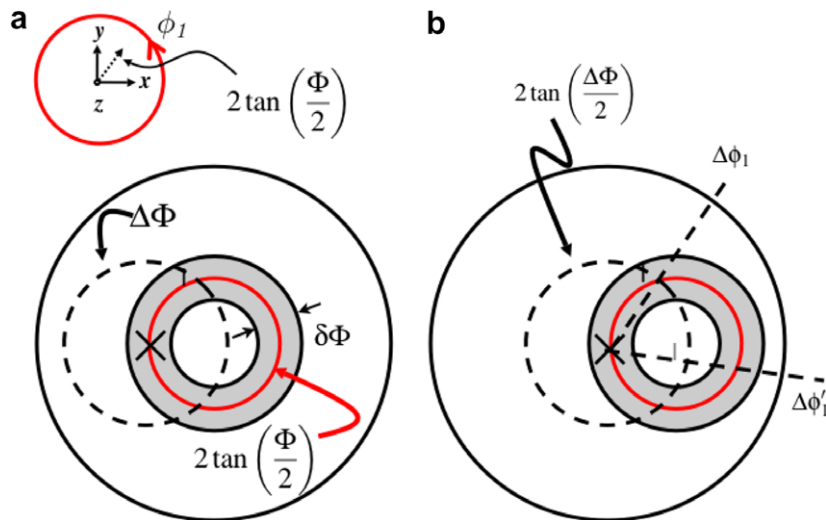


Fig. 2. (a) Geometrical depiction of a stereographic projection of a hypothetical polycrystal whose crystallographic orientations are constrained to a cone angle,  $\Phi \pm \delta\Phi/2$  (gray shaded annulus). (b) Shows the distribution of orientations from the reference system of an arbitrary grain, denoted as  $\times$ . The dashed circle denotes the locus of misorientations with fixed cone angle  $\Delta\Phi$ . For a fixed cone angle,  $\Delta\Phi$ ,  $\Delta\phi'_1$  is an unrealizable misorientation ( $\Delta\vec{g}' = \Delta\vec{g}'(\Delta\phi'_1, \Delta\Phi)$  is impossible), while the polar angle  $\Delta\phi_1$  has a finite probability (i.e.,  $\Delta\vec{g} = \Delta\vec{g}(\Delta\phi_1, \Delta\Phi)$  is possible).

misoriented by  $\Delta\Phi$  are denoted by the intersection of the dashed circle of radius  $2\text{tan}(\Delta\Phi/2)$  with the shifted ring.

Therefore, the shape of the ODF influences the accessible values of misorientation that an arbitrary pair of grains can reach, i.e., specifies the range of possible MDFs. For example, from Fig. 2b, the misorientation  $\Delta\vec{g}_{ij} = \Delta\vec{g}_{ij}(\Delta\phi_1, \Delta\Phi)$  has a finite probability of occurring, while the misorientation  $\Delta\vec{g}'_{ij} = \Delta\vec{g}'_{ij}(\Delta\phi'_1, \Delta\Phi)$  has zero probability. However, pairs of grains with a misorientation angle  $\Delta\phi'_1$  are likely if  $\Delta\Phi$  is made large (or small) enough to belong to the imposed ODF. Similarly, for a fixed value of  $\Delta\phi_1$ , a range of misorientation values for  $\Delta\Phi$  is available.

## 2.2. Mathematical representation

The geometrical construction of Section 2.1 can be mathematically described for a polycrystal of total volume  $\Omega$ , whose grain size is uniform and morphologically isotropic. The probability of finding a pair of volume elements whose associated grains (arbitrarily labeled 1 and 2) have crystallographic orientations  $\vec{g}_1$  and  $\vec{g}_2$ , related by a misorientation  $\Delta\vec{g}$ , with position vectors  $\vec{x}_1$  and  $\vec{x}_2$ , and separated by the position vector,  $\vec{\Delta x}$  is given by (see Fig. 3):

$$P_M(\vec{t}_O, \vec{g}_1, \vec{g}_2, \vec{x}_1, \vec{x}_2) = P_O(\vec{t}_O, \vec{g}_1, \vec{x}_1)P_O(\vec{t}_O, \vec{g}_2, \vec{x}_2) \quad (3)$$

or in more explicit terms:

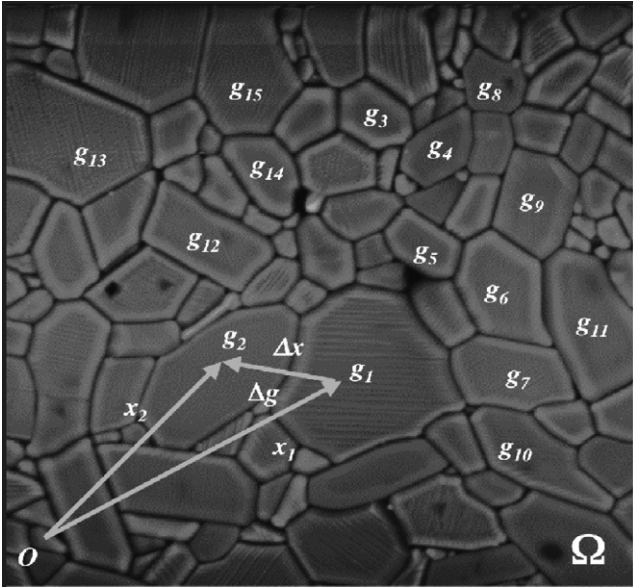


Fig. 3. Example of a polycrystal with volume  $\Omega$  and unspecified (correlated) spatial distribution of crystallographic orientations. For a fixed arbitrary laboratory reference system origin,  $\theta$ , two neighboring grains at positions  $\vec{x}_1$  and  $\vec{x}_2$ , with orientations  $\vec{g}_1$  and  $\vec{g}_2$ , separated by a distance vector  $\vec{\Delta x}$  will have a misorientation  $\Delta\vec{g}$ . The ensemble of crystallographic orientations,  $\vec{g}_1 \dots \vec{g}_N$ , i.e., the ODF, constrains the statistically accessible misorientations (MDF). Micrograph courtesy of Jay Wallace.

$$P_M(\vec{t}_M, \vec{g}_1, \Delta\vec{g}, \vec{x}_1, \vec{\Delta x}) = P_O(\vec{t}_O, \vec{g}_1, \vec{x}_1)P_O(\vec{t}_O, \Delta\vec{g} \cdot \vec{g}_1, \vec{x}_1 + \vec{\Delta x}) \quad (4)$$

Eq. (4) illustrates that the probability of misorientation of two grains, i.e., the MDF, is the product of the position-dependent ODFs.

Assume that the position-dependent ODF can be separated into its spatial and orientation components:

$$P_O(\vec{t}_O, \vec{g}, \vec{x}) = P_O(\vec{t}_O, \vec{g})S(\vec{x}) \quad (5)$$

$P_O(\vec{t}, \vec{g})$  is the spatially independent orientation probability distribution function, as it is routinely extracted from X-ray diffraction experiments.  $S(\vec{x})$  embodies the spatial modulations of the ODF, such that  $0 \leq S(\vec{x}) \leq 1$ . So, for a fixed value of  $\vec{g}$ , those regions in the polycrystal where  $S(\vec{x}) = 0$  have zero likelihood of contributing to  $P_O(\vec{t}, \vec{g}, \vec{x})$ , while those regions with a value of  $S(\vec{x}) > 0$  will have a finite probability.  $S(\vec{x})$  identifies those areas in a polycrystal that are textured, and distinguishes between correlated and uncorrelated orientations of grains that may result during processing of the material, such as those induced by the macroscopic surfaces, chemical inhomogeneities, etc. For example, a polycrystalline material with two populations of grains, a textured and an untextured one, will have an ODF of the form:

$$P_O(\vec{t}, \vec{g}, \vec{x}) = P_O(\vec{t}_O, \vec{g})S_1(\vec{x}) + S_2(\vec{x}) \quad (6)$$

where  $S_1(\vec{x}) = 1$  for the textured volume fraction of grains,  $S_2(\vec{x}) = 1$  for the untextured volume fraction, and  $S(x) = S_1(x) + S_2(x) = 1$ . The spatial contribution of those grains is such that:

$$v = \int_{\Omega} S_1(\vec{x})d\vec{x} \quad (7)$$

$v$  is the textured volume fraction of grains, and  $\Omega$  is the volume of the polycrystal.

By substituting Eq. (5) into Eq. (4), the probability of finding two grains, one at an orientation  $\vec{g}_1$ , a second misoriented by  $\Delta\vec{g}$ , and separated by  $\Delta x$  apart, for all positions in a polycrystal is:

$$P_M(\vec{t}, \vec{g}_1, \Delta\vec{g}, \vec{\Delta x}) = \int_{\Omega} S(\vec{x})S(\vec{x} + \vec{\Delta x})P_O(\vec{t}, \vec{g}_1)P_O(\vec{t}, \Delta\vec{g} \cdot \vec{g}_1)d\vec{x} = P_O(\vec{t}, \vec{g}_1)P_O(\vec{t}, \Delta\vec{g} \cdot \vec{g}_1)\mathcal{C}(\vec{\Delta x}) \quad (8)$$

where

$$\mathcal{C}(\vec{\Delta x}) = \int_{\Omega} S(\vec{x})S(\vec{x} + \vec{\Delta x})d\vec{x} \quad (9)$$

is the degree of correlation between two points in a polycrystal.  $\mathcal{C}(\vec{\Delta x})$  modulates the probability of finding two grains at misorientation,  $\Delta\vec{g}$ , separated by  $\vec{x}$ . The specific form of  $\mathcal{C}(\vec{\Delta x})$  depends on the average correlation between grains surrounding a central representative one. For example, for a hypothetical polycrystal, the step function

$\mathcal{C}(|\vec{\Delta x}|) = C_0 \Omega / L^3$ , for  $\Delta x < L$ , and  $\mathcal{C}(|\vec{\Delta x}|) = 0$ , for  $\Delta x > L$ , provides a measure of correlated grains a distance  $L$  away from each other.  $C_0$  is a normalizing factor. If  $L$  is much smaller than the characteristic grain size, then the polycrystal is an ensemble of spatially uncorrelated grains. If  $L$  is on the order of the grain size, then only neighboring grains are spatially correlated and make contributions to the MDF. Finally, if  $L$  is of the order of the macroscopic characteristic length scale, then all the orientations of all the grains are spatially correlated.

An expression that describes the misorientation probability distribution for neighboring grains is obtained by starting from Eq. (8) and it considers the contributions from all the grains, at all orientations,  $\vec{g}_1$ , at a fixed distance  $\Delta x$ , and misorientation  $\Delta \vec{g}$ :

$$P_M(\vec{t}, \Delta \vec{g}, \vec{\Delta x}) = \mathcal{C}(\vec{\Delta x}) \int_{\vec{g}} P_O(\vec{t}, \vec{g}_1) P_O(\vec{t}, \Delta \vec{g} \cdot \vec{g}_1) d\vec{g}_1 \quad (10)$$

The grain–grain correlations necessary to solve Eq. (10) can be extracted from EBSD diffraction experiments. In the absence of such information, a numerically useful relation between the ODF and MDF of a polycrystal is obtained by determining the probability of finding an arbitrary pair of grains, independent of their separation in the polycrystal, one with a fixed orientation  $\vec{g}_1$ , and the other at a misorientation  $\Delta \vec{g}$ :

$$P_M(\vec{t}, \vec{g}_1, \Delta \vec{g}) = \mathcal{M} P_O(\vec{t}, \vec{g}_1) P_O(\vec{t}, \Delta \vec{g} \cdot \vec{g}_1) \quad (11)$$

with

$$\mathcal{M} = \int_{\Omega} \mathcal{C}(\vec{\Delta x}) d\vec{\Delta x} = \int_{\Omega} \int_{\Omega} S(\vec{x}) S(\vec{x} + \vec{\Delta x}) d\vec{x} d\vec{\Delta x} \quad (12)$$

and is defined as the microstructure factor.  $\mathcal{M}$  sums up all the spatial correlations between all positions and spatial separations within the volume  $\Omega$ . In the limit of a polycrystal where two arbitrary points are statistically equivalent ( $S(\vec{x}) = 1/\Omega$ ),  $\mathcal{M} = 1$ .

For a fixed orientation  $\vec{g}_1$ , there is a finite number of interfaces at a misorientation  $\Delta \vec{g}$ ; therefore, the probability of sampling a specific misorientation for all possible values of orientation  $\vec{g}_1$  is given by the expression:

$$P_M(\vec{t}, \Delta \vec{g}) = \mathcal{M} \int_{\vec{g}} P_O(\vec{t}, \vec{g}_1) P_O(\vec{t}, \Delta \vec{g} \cdot \vec{g}_1) d\vec{g}_1 \quad (13)$$

which is readily proposed by Zhao et al. [25], without detailed justification. Eq. (13) states that the probability of misorientation constrains (and is constrained by) the ODF. Therefore, microstructural designs that favor the occurrence of a specific set of microstructural interfaces are equivalent to texture designs where the orientation of one or more crystallographic axes are preferred. In the limit of  $\mathcal{M} \rightarrow 1$ , Eq. (13) is defined as the maximal MDF, and does not distinguish between misorientations sampled for pairs of grains sharing a common interface or at opposite extremes in the solid. The spatial contributions to the MDF are specified through  $\mathcal{C}(\vec{\Delta x})$ , and together with the maximal MDF fully characterize the polycrystal. The max-

imal MDF is an upper bound of an experimentally determined MDF, which measures the orientation correlations between neighboring grains only.

In the following section, the theoretical framework described herein is applied to predict the impact of a well-known analytical expression of fiber texture on the maximal misorientation probability distribution.

### 3. Application to a fiber-textured solid

For a solid possessing fiber texture,  $\Phi$  is the angle made by the textured crystallographic axis and the fiber axis, a cone angle, whose values range between 0 and  $\pi$ . The March orientation probability distribution predicts the probability of finding a specific crystal direction of a grain, e.g., the  $c$ -axis, at a cone angle between  $\Phi$  and  $\Phi + d\Phi$  away from the textured axis [19,20]:

$$P_f(r, \Phi) = \frac{1}{4\pi} \frac{\sin \Phi}{(r^2 \cos^2 \Phi + \frac{1}{r} \sin^2 \Phi)^{3/2}} \quad (14)$$

Assume the fiber axis is aligned with the  $z$ -axis of the laboratory reference system, as described in Fig. 1. Values of  $r$  range from 0 to  $\infty$ . The present paper is concerned with values of  $r$  ranging from 0 to 1, which find applications, among other processes, in tape casting and film deposition. A limiting value of  $r = 0$  indicates perfect texture: the preferred orientation direction of each grain is perfectly parallel or antiparallel with the fiber axis. A value of  $r = 1$  signifies complete randomness, or no texture (see Fig. 4).

The maximal MDF is calculated by directly substituting Eq. (14) into Eq. (13). For  $r = 0.3$ , results are summarized in Fig. 5. Two significant misorientation populations are predicted, a larger one close to  $\Delta \Phi = \pi$ ,  $\Delta \phi_1 = 0$  and  $\pi$ , and a smaller one close to  $\Delta \Phi = 0$ ,  $\Delta \phi_1 = \pm \pi/2$ . These two populations of misorientation angles are a result of the two most probable cone angles that the March distribution function generates. From the reference system of an arbitrary grain obeying Eq. (14), the first population of grains will have orientations very close to each other, i.e., sharing essentially the same cone angle (parallel to each other), and the only difference between them is the value of the polar angle,  $\phi_1$ . The second population of grains is roughly oriented at a cone angle of  $\pi$  radians (antiparallel) with respect to the randomly selected central grain of the first population, and the only difference between the orientations of the second population is the value of polar angle. For both populations, the values of polar angles range from zero to  $\pm \pi$ , and low polar angle values are favored with respect to large ones. As a result of such behavior, the misorientation of the  $c$ -axes between two arbitrary grains will be either very small or very large.

The calculations presented herein distinguish between those grains whose  $c$ -axes are misoriented by  $\pi$  radians. In general, the crystal structure of a grain imposes restrictions on the distinguishable crystallographic misorientations that can be sampled. For example, for those polycrystals with an inherent center of inversion, the

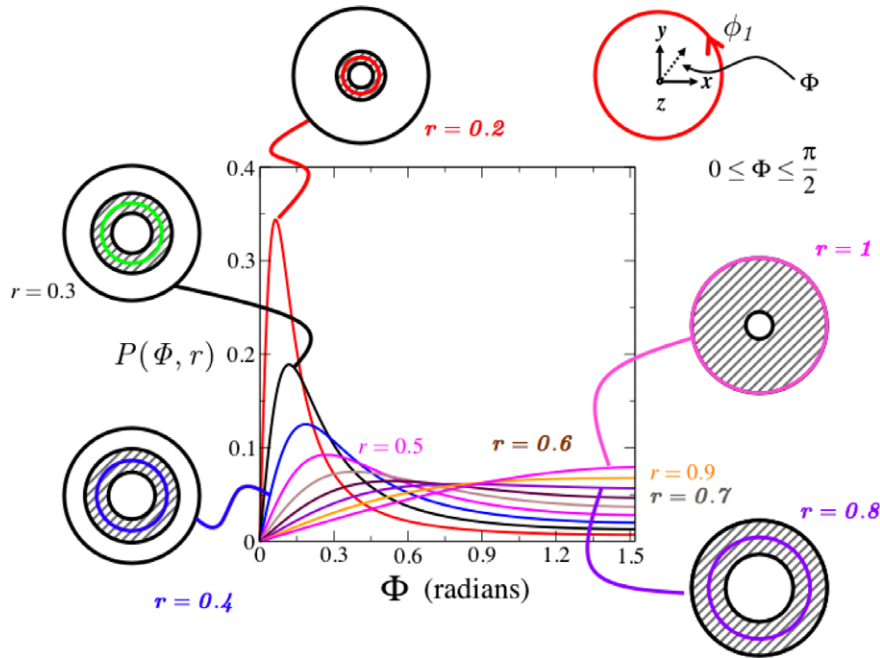


Fig. 4. March orientation probability distribution as a function of orientation,  $\Phi$ , for different values of texture parameter,  $r$ . For highly textured materials,  $r \approx 0$ , small cone angles are more probable to be sampled than large ones. However, as the value of texture decreases, i.e., as  $r \rightarrow 1$ , larger values of cone angles are more probable, while small angle values are less likely to be sampled. In the limit of  $r = 1$ , the average cone angle is  $\Phi = \pi/2$ , and all cone angles occur with a probability  $P(r = 0, \Phi) = \sin\Phi$ . The most probable cone angle and its dispersion is illustrated through a sketch of the associated pole figure.

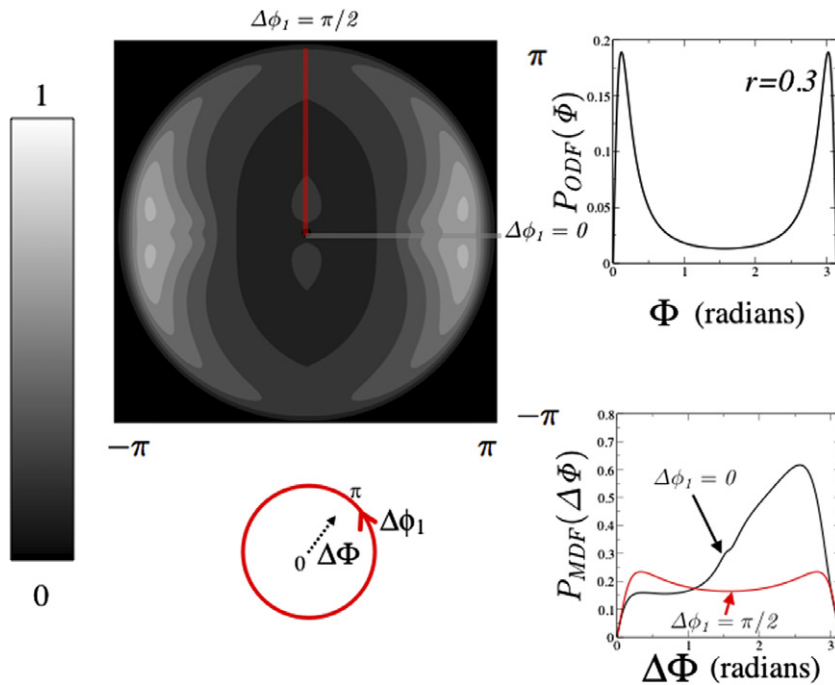


Fig. 5. Top left: polar plot of the maximal misorientation probability distribution of the March function, for  $r = 0.3$ . The two-dimensional radial direction takes values of  $\Delta\Phi$  between 0 and  $\pi$ . The angular direction,  $\Delta\phi_1$  corresponds to the polar direction, and takes values between 0 and  $2\pi$ . The key to the probability density map is shown on the left. Bottom left: the key to the two-dimensional map. Radial direction corresponds to  $\Delta\Phi$  and angular direction to  $\Delta\phi_1$ . Top right: March orientation probability distribution, for  $r = 0.3$  (see Eq. (14)). Bottom right: MDF as a function of  $\Delta\Phi$  for two fixed values of  $\Delta\phi_1$ .

accessible values of cone angle misorientations are constrained to the range  $[0, \pi/2]$  because for such cases, the orientation of each grain does not distinguish between the

values  $\Delta\Phi = 0$  and  $\Delta\Phi = \pm \pi$ . The results shown in Section 3 are directly applicable to describing the statistics of materials whose crystal structure belong to the point group 1.

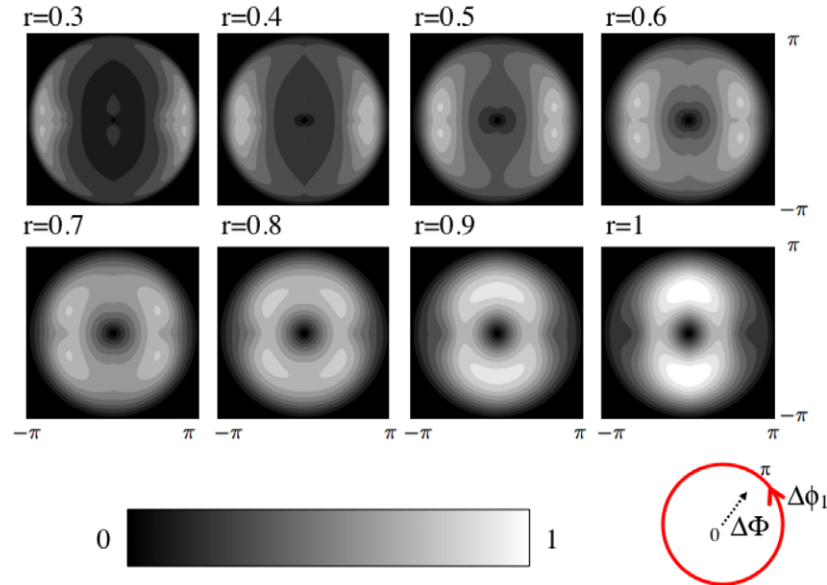


Fig. 6. Probability misorientation distribution plots for Eq. (14) for different values of texture parameter,  $r$ . For highly textured materials, cone angle misorientations,  $\Delta\Phi$ , closer to zero and  $\pi$  are more probable, while values of  $\Delta\phi_1$  closer to 0,  $\pi/2$ ,  $\pi$ , and  $3\pi/2$  are easier to access. As the randomness of the material increases, i.e., as  $r \rightarrow 1$ , intermediate values of polar and cone angles are sampled at a higher rate. In the limit of  $r = 1$ ,  $\Delta\Phi = \pi/2$ ,  $\Delta\phi_1 = \pm \pi/2$  are the most probable misorientation angles (see text for details). The key to the gray scale values is shown at the bottom. The key to the orientational dependence of the MDF plot is shown at the bottom right.

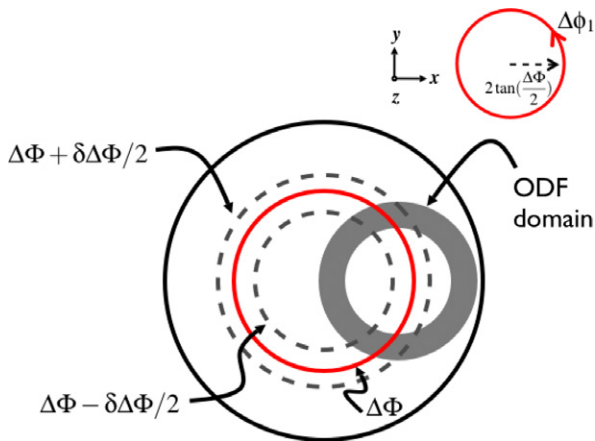


Fig. 7. Schematic depiction of the effect of a fiber-textured material on the associated maximal MDF. The probability of finding a cone angle misorientation between  $\Delta\Phi - \delta\Delta\Phi/2$  and  $\Delta\Phi + \delta\Delta\Phi/2$  is graphically illustrated by the intersected areas of the dashed ring with the filled ring (see Fig. 2). For increasing randomness, misorientations with larger values of  $\Delta\phi_1$  become more likely to sample, while small values of  $\Delta\phi_1$  become less probable.

The effect of changes in texture on the MDF is summarized in Fig. 6. In general, as the texture parameter,  $r$ , increases, the smallest most probable cone angle of the ODF increases, while the largest cone angle decreases. Also, the dispersion around both cone angles increases. As a result, intermediate cone and polar angle misorientations become more likely to be sampled. Therefore, as a polycrystal becomes increasingly random, the two populations of most probable misorientations approach each other. In the limit of no texture,  $r = 1$ , the two populations

of cone angles become indistinguishable. Furthermore, the polar angle misorientations,  $\Delta\phi_1 = \pm \pi/2$ , become more likely to occur than other values, and the cone angle misorientation  $\Delta\Phi = \pi/2$  is the most probable; moreover, even though all the crystallographic orientations are equally probable, all the crystallographic misorientations are not.

Graphically, the effect of fiber texture on the maximal MDF is illustrated in Fig. 7.

Here, the accessible misorientations with cone angles between  $\Delta\Phi - \delta\Delta\Phi/2$  and  $\Delta\Phi + \delta\Delta\Phi/2$  correspond to the intersection of the dashed ring and the filled ring in the stereographic projection plane (e.g., Fig. 7). For a polycrystal satisfying Eq. (14), as the degree of texture in the polycrystal decreases, the radius and the thickness of the filled ring increases, thus greater values of  $\Delta\phi_1$  are intersected, while making small values of  $\Delta\phi_1$  less likely to occur. Furthermore, the values of cone angle misorientations that can be sampled become larger with decreasing texture, and the probability of sampling small values of polar angle misorientations decreases. This process makes intermediate values of cone and polar angle misorientations more probable and contributions from an intermediate region less probable.

#### 4. Summary and conclusions

A complete statistical description of polycrystalline materials includes the orientation, misorientation, the interface normals distribution, as well as the degree of morphological texture that a solid may exhibit. For morphologically isotropic materials, orientation and misorientation probability distributions are correlated functions,

and the spatially dependent misorientation distribution function is the product of the maximal MDF and the degree of correlation factors. The maximal MDF is an upper bound of the observable set of misorientations. The derivation presented in this manuscript demonstrates that the parameters needed to fully characterize the MDF are the same parameters required to accurately determine the ODF.

The calculations presented in this paper show that the probability of misorientation between two grains is constrained by the statistics of the neighboring crystallographic orientations that the grains can reach. The present analysis outlines a methodology that can be extended to specify the character of more complex microstructural features, such as triple junctions, and thus correlate the impact that these microstructural features may have on the properties of the system.

The framework presented in Section 2, and results in Section 3 demonstrate that processing techniques where a subset of grain misorientations is favored are equivalent to inducing a specific type of macroscopic texture. Therefore, interface engineering methods are equivalent to tailoring the texture of polycrystalline materials. For the selected representation of fiber texture (the March function), a subset of polar and cone angle misorientations is favored by samples where the texture parameters are judiciously selected. For highly oriented fiber-textured materials, low-angle misorientations are statistically favored with respect to high-angle misorientations. High-angle misorientations become more probable as texture decreases; however, for materials exhibiting no texture, small-angle misorientations are less likely to occur than large-angle misorientations. For point group 1 materials, calculations suggest that two types of misorientations can be preferentially sampled: small polar, large cone angle boundaries,  $\Delta \vec{g} = \Delta \vec{g}(\Delta\phi_1 = 0, \Delta\Phi = \pi/2)$ , and large polar, small cone angle boundaries,  $\Delta \vec{g} = \Delta \vec{g}(\Delta\phi_1 = \pm\pi/2, \Delta\Phi = 0)$ . The two populations are distinguishable for highly textured solids. As the degree of texture decreases, the polar angle misorientation distribution becomes less pronounced. However, in the limit of a completely random solid,  $\Delta \vec{g} = \Delta \vec{g}(\Delta\phi_1 = \pm\pi/2, \Delta\Phi = \pi/2)$  is more likely to be sampled than those misorientations with  $\Delta\phi_1 = 0$ .

## References

- [1] Rhorer GS, Saylor DM, Dasher BE, Adams BL, Rollet AD, Wynblatt P. The distribution of internal interfaces in polycrystals. *Int J Mater Res Adv Techniques B (basic)* 2004;95:1–18.
- [2] Saylor DM, Dasher BE, Sano T, Rorher GS. Distribution of grain boundaries in SrTiO<sub>3</sub> as a function of five macroscopic parameters. *J Am Ceram Soc* 2004;87:670–6.
- [3] Sabolsky EM, Messing GL, Trolier-McKinstry S. Kinetics of templated grain growth of 0.65Pb(Mg<sub>1/3</sub>Nb<sub>2/3</sub>O<sub>3</sub>·0.35PbTiO<sub>3</sub>). *J Am Ceram Soc* 2001;84:2507–13.
- [4] Heinz A, Neumann P. Representation of orientation and disorientation data for cubic, hexagonal, tetragonal and orthorhombic crystals. *Acta Cryst* 1991;A47:780–9.
- [5] Frank FC. The 1987 institute of metals lecture. The metallurgical society: orientation mapping. *Metall Trans A* 1988;19:403–7.
- [6] Moraweic A, Field DP. Rodrigues parameterization for orientation and misorientation distributions. *Philos Mag A* 1996;73:1113–30.
- [7] Fuller E. Microstructural stresses: structural reliability and antiquity preservation. In: Robert B. Sosman Lecture, 106th annual meeting of the American ceramic society, Indianapolis, IN, April 21, 2004.
- [8] McKenzie JK. *Biometrika* 1958(45):229.
- [9] Lee PS, Piehler HR, Rollet AD, Adams BL. Texture clustering and long-range disorientation representation methods: application to 6022 aluminum sheet. *Metall Trans A* 2002;33:3709.
- [10] Gao X, Przybyla CP, Adams BL. Methodologies for recovering and analyzing two-point pair correlation function in polycrystalline materials. *Metall Mater Trans A* 2006;37A:2379–87.
- [11] Frary M, Schuh CA. Grain boundary networks: scaling laws, preferred cluster structure and their implications for grain boundary engineering. *Acta Mater* 2005;53:4323–35.
- [12] Schuh CA, Minich RW, Kumar M. Connectivity and percolation in simulated grain boundary networks. *Philos Mag* 2003;A83:711–26.
- [13] Minich RW, Schuh CA, Kumar M. The role of topological constraints on the statistical properties of grain boundary networks. *Phys Rev B* 2002;66:052101.
- [14] Bunge H-J. *Texture analysis in materials science*. London: Butterworth; 1993.
- [15] Randall RV, Engler O. *Introduction to texture analysis: macrotexture, microtexture, and orientation mapping*. Amsterdam: Gordon and Breach; 2000.
- [16] Moraweic A. *Orientations and rotations*. New York: Springer; 2003.
- [17] March A. *Mathematische theorie der regelung nach der korgestalt bei affiner deformation*. *Z Kristallogr* 1932;81:285–97.
- [18] Dollase WA. Correction of intensities for preferred orientation in powder diffractometry: application of the March model. *J Appl Crystallogr* 1986;19:267–72.
- [19] Zhao J, Adams BL, Morris PR. A comparison of measured and textured-estimated misorientation distributions in type 304 stainless steel tubing. *Texture Microstruct*. London: Gordon and Breach; 1987. p. 0–16.